THE ASTROPHYSICAL JOURNAL, 538:307–314, 2000 July 20

THE TIMING EVOLUTION OF 4U 1630−47 DURING ITS 1998 OUTBURST

S. W. DIETERS,[1,2] T. BELLONI,[3] E. KUULKERS,[4] P. WOODS,[1,2] W. CUI,[5] S. N. ZHANG,[1] W. CHEN,[6] M. VAN DER KLIS,[7] J. VAN PARADIJS,[1,7] J. SWANK,[6] W. H. G. LEWIN,[5] AND C. KOUVELIOTOU[2,8]

Received 1999 September 27; accepted 2000 February 28

ABSTRACT

We report on the evolution of the timing of 4U 1630−47 during its 1998 outburst using data obtained with the *Rossi X-ray Timing Explorer* (*RXTE*). The count rate and position in hardness intensity, color-color diagrams, and simple spectral fits are used to track the concurrent spectral changes. The source showed seven distinct types of timing behavior, most of which show differences with the canonical black hole spectral/timing states. In marked contrast to previous outbursts, we find quasi-periodic oscillation (QPO) signals during nearly all stages of the outburst with frequencies between 0.06 and 14 Hz and a remarkable variety of other characteristics. In particular, we find large (up to 23% rms) amplitude QPOs on the early rise. Later, slow 0.1 Hz semiregular short (∼5 s), 9%–16% deep dips dominate the light curve. At this time there are two QPOs, one stable near 13.5 Hz and the other whose frequency drops from the 6–8 Hz range to ∼4.5 Hz during the dips. *BeppoSAX* observations during the very late declining phase show 4U 1630−47 in a low state.

Subject headings: accretion, accretion disks — binaries: close — stars: individual (4U 1630−47) — X-rays: stars

1. INTRODUCTION

4U 1630−47 has shown recurrent X-ray outbursts with intervals of 600–700 days (Jones et al. 1976; Priedhorsky 1986; Kuulkers et al. 1997a). This is much shorter than the typical waiting time of 10–50 yr for soft X-ray transients (Tanaka & Lewin 1995), which makes 4U 1630−47 an important source for studying how the spectral/timing behavior depends upon mass accretion rate and/or other parameters.

4U 1630−47 is a black hole candidate (Parmar, Stella, & White 1986; Barret, McClintock, & Grindlay 1996; Kuulkers et al. 1997a) because it has shown spectral and timing characteristics similar to those of other X-ray sources with a measured high mass function. The X-ray behavior of black hole candidates (BHCs) is usually classified into four timing/spectral states, which are in order of increasing 2–10 keV X-ray flux and presumably mass accretion rate: low, intermediate, high, and very high states (see van der Klis 1995; Cui 1999). An alternative view of the various states is given by Rutledge et al. (1999). In the low state (LS), the power density spectrum (PDS) shows strong (30%–50% rms) band-limited (flat topped) noise with a break between 0.03 and 0.3 Hz, and the energy spectrum is well fit with a power law with index of $\Gamma = -1.5$ to -2.5 up to at least 200 keV (Gilfanov et al. 1994). In the high state (HS), the PDS shows weak (few percent rms) power-law noise. The energy spectrum is dominated by a soft component that can be satisfactorily fit by a multitemperature disk blackbody. The fitted temperature ($kT \sim 1$ keV) and innermost radius are comparable to values expected for a stellar-mass black hole. In the very high state (VHS), the soft component increases in flux by a further factor of 2–8 over that in the high state. The power-law component strengthens and is visible in the energy spectra. The power density spectrum shows a variable broadband component and 3–10 Hz quasi-periodic oscillation (QPO). The noise component is either band-limited with a break between 1 and 20 Hz or a power law similar to that in the high state. Occasionally at times between an HS and an LS, an intermediate state (IS) is observed, e.g., GX 339−4 (Méndez & van der Klis 1997), GS 1124−68 (Belloni et al. 1997a), GRO J1655−40 (Méndez, Belloni, & van der Klis 1998), and Cyg X-1 (Belloni et al. 1996; Cui et al. 1997). The intermediate state has fluxes and spectral properties intermediate to those of the HS and LS. The power spectral properties are very much like the VHS. Slow, less than 1 Hz, QPOs have been observed in all states.

4U 1630−47 has quite variable outbursts. The 1996 outburst lasted ∼50 days, the 1977 outburst lasted ∼10 months, and the 1988–1991 interval showed ongoing long-term activity (Kuulkers, van der Klis, & Parmar 1997b). Even though the 1987 and 1996 outbursts had similar flux histories, they show opposite trends in spectral hardness as a function of time (Kuulkers et al. 1997a). Such a range in behavior is akin to the variety of outbursts of the superluminal jet sources GRS 1915+105 and GRO 1655−40.

There are other similarities between 4U 1630−47 and these sources. During the 1998 outburst, radio emission was detected just as the source was making a transition from hard to soft emission (Hjellming et al. 1999). This is very similar to the behavior of GRS 1739−278 and jet sources.

[1] Postal address: University of Alabama in Huntsville, 301 Sparkman Drive, Huntsville, AL 35899.
[2] NASA/Marshall Space Flight Center, SD-50, Huntsville, AL 35812; stefan.dieters@msfc.nasa.gov, pete.woods@msfc.nasa.gov, shuang.zhang@msfc.nasa.gov, and chryssa.kouveliotou@msfc.nasa.gov.
[3] Osservatorio Astronomico di Brera, Via E. Bianchi 46, I-23807, Merate (LC), Italy; belloni@merate.mi.astro.if.
[4] Space Research Organization Netherlands, Sorbonnelaan 2, 3584 CA, Utrecht, The Netherlands; also Astronomical Institute, Utrecht University; erikk@sron.nl.
[5] Massachusetts Institute of Technology, Center for Space Research, Cambridge, MA 02139; cui@aqlxl.mit.edu, lewin@space.mit.edu.
[6] NASA/Goddard Space Flight Center, Code 661, Greenbelt, MD 20771; chen@milkyway.gsfc.nasa.gov, swank@milkyway.gsfc.nasa.gov.
[7] Astronomical Institute "Anton Pannekoek," University of Amsterdam, Kruislaan 403, 1098 SJ Amsterdam, The Netherlands; michiel@astro.uva.nl.
[8] Universities Space Research Association.

Also, 4U 1630−47 showed strong linear polarization in its radio flux, which has only been observed from elongated jet sources like SS 433, GRS 1915+105, and GRO 1655−40 (Hjellming et al. 1999 and references therein).

Absorption dips lasting 50–150 s and reaching 8%–30% of the nondip flux have been observed from 4U 1630−47 (Kuulkers et al. 1997b; Tomsick, Lapshov, & Kaaret 1998). These dips indicate that, like GRO 1655−40 and the accretion disk corona sources, 4U 1630−47 is being viewed at a high (60°–75°) inclination. This cannot be confirmed since no optical counterpart has so far been identified (Parmar et al. 1986; M. Buxton 1998, private communication). It is expected that these absorption dips will occur over a restricted range in phase and so yield an estimate of the orbital period. We find no evidence for any absorption dips in our data.

The 1998 outburst began with a slow rise in the 20–100 keV (BATSE) flux starting near January 28 (TJD 10,841; TJD = JD − 2,440,000.5). Later, on February 3 (TJD 10,847) the *Rossi X-ray Timing Explorer* (*RXTE*) all-sky monitor (ASM) (Levine et al. 1996) began showing 2–12 keV flux. Radio emission is thought to have started just as soft flux began its rapid rise near February 7 (TJD 10,851). *RXTE* PCA observations were triggered at this time. This outburst was well covered (100 observations) by *RXTE* (this paper; Tomsick & Kaaret 2000), *ROSAT* HRI/PSPC (between February 17 and 28), *BeppoSAX* (Oosterbroek et al. 1998), *ASCA* (February 25–26), and BATSE and radio (Hjellming et al. 1999). In this paper we discuss the evolution of the timing behavior during the 1998 outburst.

Between 1999 May and September, well in advance of its next expected outburst (1999 mid-December; Kuulkers et al. 1998), 4U 1630−47 underwent a fainter than normal outburst. In terms of the very early flux evolution in the BATSE and *RXTE* ASM energy ranges, the 1999 outburst was almost identical to that in 1998. On the very early rise (1999 May 8), a single 0.85 Hz, 16% rms QPO peak was found in the power density spectrum (McCollough et al. 1999). At this time the energy spectrum was hard. An observation 2 days later failed to find any QPO.

2. OBSERVATIONS

The observations discussed here (Observation ID: 30178-0[1-2]- and 30188-02-) were taken with the *RXTE* PCA (Jahoda et al. 1996) roughly daily, beginning on 1998 February 9, until 4U 1630−47 reached maximum on February 22. After maximum our observations were made every 2–5 days until 1998 March 31. Observations that partially overlap ours and extend until 1998 June 8 are reported by Tomsick & Kaaret (2000).

We analyzed 49 observations, most of which are ∼1.4 ks in length. For each of the pointings, we calculated power density spectra from segments of data 1, 2, 16, and 256 s long, using the whole energy range of 2–60 keV. The time resolution used is mostly 2 ms. Power spectra were selected by time and intensity so that the resulting average spectra are representative of the different flux levels within each observation. In many observations the count rate did not vary much, and one average power density spectrum was sufficient to characterize the observation. The averaged power density spectra were normalized to the rms variability (Belloni & Hasinger 1990) using the average background as estimated using PCABACKEST V2.1b and corrected for PCA dead time (Zhang et al. 1995; Zhang 1995).

The average count rate, two hardness ratios, and pulse-height analyzer (PHA) spectra were determined for each observation using Standard 2 mode data from only a single PCA detector (PCU 0). Data selection and background subtraction followed standard procedures.

In addition, we present two serendipitous *BeppoSAX* observations made with the Medium Energy Concentrator Spectrometer (MECS) (Boella et al. 1997) on 1998 August 7 (TJD 11,032) and 1998 September 16 (TJD 11,072). *BeppoSAX* was pointed at SGR 1621−47, placing 4U 1630−47 at the edge of the field of view with an offset of 22′. The on-source times were 85.7 and 62.4 ks, respectively. Source counts were collected from a 30′ diameter circle that included the entire elongated image of 4U 1630−47. Background counts were extracted from a circular patch of the same size centered at the same offset on the opposite side of the MECS field of view. The response matrix was that for a 20′ offset. The expected resulting systematic errors on the spectrum are 5%–10%.

3. RESULTS

During the outburst, seven distinct types of timing behavior occurred. We label the different behaviors as A, B (b), C, D, E, F, and G. The distinctions are primarily in the shape of the broadband noise and secondarily in the properties of the QPO. The timing properties change hand in hand with changes in the energy spectrum. Figure 1 gives an overview of the count rate and spectral changes as represented by two light curves, a hardness intensity, and a color-color diagram. Figure 2 shows from our data five representative power density spectra (behaviors A, B, C, D, and E), whose fit parameters are given in Table 1.

3.1. *Timing Properties*

Behavior A.—During the first *RXTE* observation (1998 February 9, TJD 10,854) while 4U 1630−47 was in the initial stages of its rise to maximum, a pair of very strong (25% and 5.6% rms) QPOs were discovered in the power density spectrum (Dieters et al. 1998a) at frequencies of 2.67 and 5.62 Hz, respectively. These are the first QPOs found from this source (except the marginal detection of Kuulkers et al. 1998), and they are among the largest amplitude QPOs ever measured from a BHC (see Fig. 2*a*). Similar large-amplitude QPOs were observed in the second observation. The power density spectra were fit with three Lorentzians to describe the peaks and a broken (flat topped) power law to describe the broadband noise. The lower frequency peak was asymmetric with a shoulder toward higher frequencies. A Lorentzian was used to fit this shoulder. The central frequencies of the two QPOs are not formally consistent with the peaks being harmonically related, but the frequencies are commensurate to well within the widths of the QPO peaks. The quality factor Q (ratio of frequency to FWHM) is 12 and 8 in the first and second observations for the lower frequency QPOs and 3–5 for the shoulder and upper frequency QPO. Between the first two observations, the count rate increased by a factor of 1.26, the QPO frequencies increased (lower QPO: 2.67 to 3.20 Hz; upper QPO: 5.62 to 6.66 Hz), the amplitude of the QPOs decreased (lower QPO: 17.03% to 15.29% rms; upper QPO

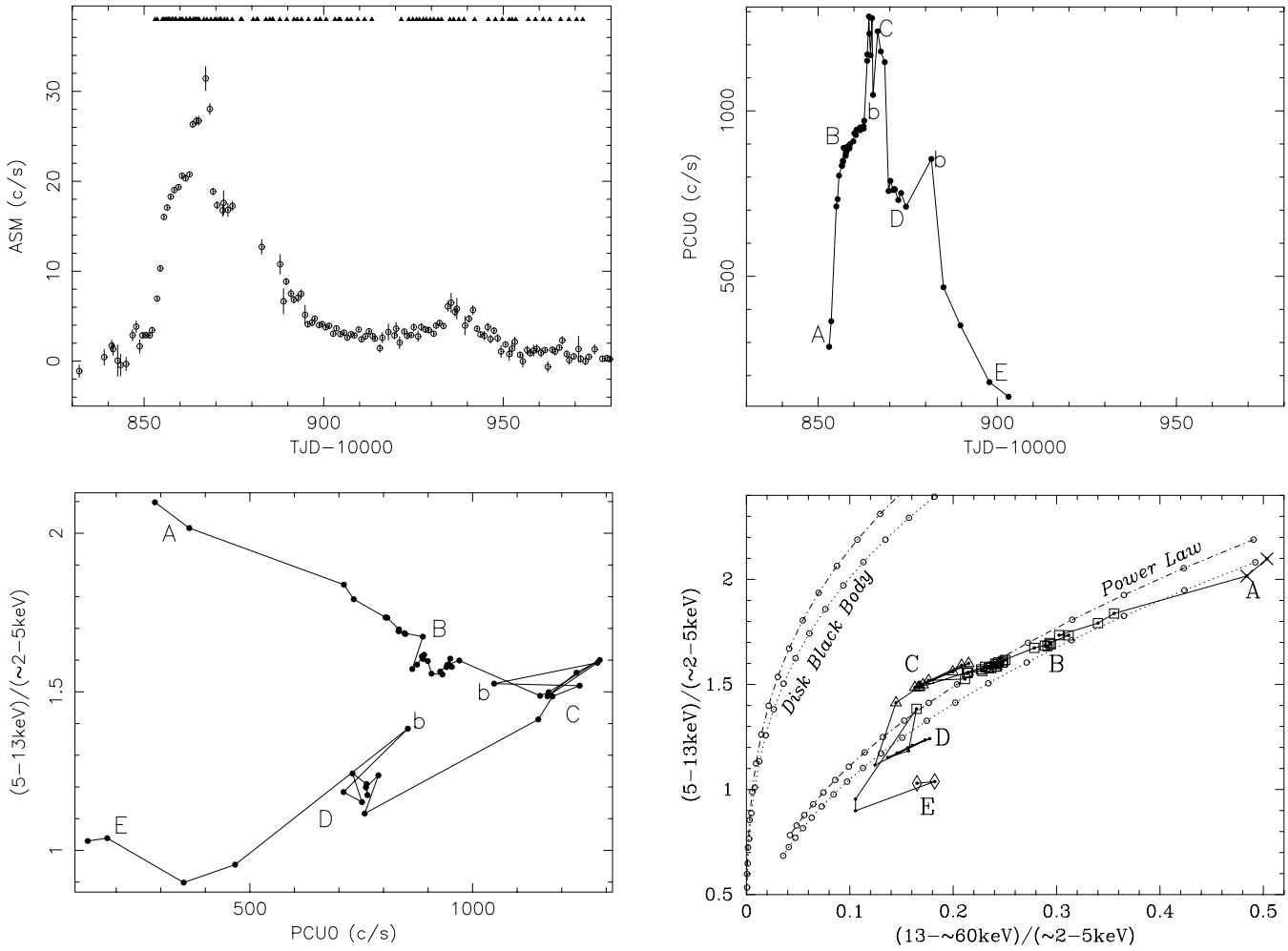

FIG. 1.—Left-hand panels show the ASM and PCA light curves for the 1998 outburst. On the ASM light curve (*top left panel*), the times of all pointed observations are marked. The PCA count rates (*lower left panel*) are the background-subtracted rates, over the full energy range (~2–~60 keV). The two right-hand panels show the hardness intensity and color-color diagrams. The count rates and hardness ratios are from PCU 0 only. The positions of the various timing/spectral behaviors are labeled, as in the text A, B, C, D, and E. Label "b" indicates the reappearance of the dipping behavior of B. In the color-color diagram, two sets of theoretical curves are shown: for a pure disk blackbody and for a pure power law. Two different absorptions are shown: $N_H = 8 \times 10^{22}$ (*dotted line*) and $N_H = 10 \times 10^{22}$ atoms cm^{-2} (*dot-dashed line*). As a reference, the rightmost points for the power-law model correspond to a photon index of 2.2 for $N_H = 8$ and 2.3 for $N_H = 10$. The other points steepen in steps of 0.1 and go until $\gamma = 4.0$. The disk blackbody points close to $Y = 1.0$ are $kT = 1.4$ ($N_H = 8$) and $kT = 1.3$ ($N_H = 10$).

5.79% to 4.16% rms), the amplitude of the broadband noise remained roughly constant at 20% rms, and the break frequency increased from 0.67 ± 0.03 to 0.94 ± 0.06 Hz. It must be noted that the break frequency depends upon which model is used to fit the broadband noise. However, the increasing trend is unchanged.

Behavior B.—After the first two observations, there was a 1 day gap in *RXTE* observations, during which 4U 1630−47 brightened rapidly (Fig. 1). Between TJD 10,856 and TJD 10,864, 4U 1640−47 continued to brighten but at an ever decreasing rate, forming a "shoulder" in the overall light curve. Short, sharp dips appeared. These dips were generally triangular in shape with a sharp drop (≤ 1 s) followed by a rise lasting 3–5 s. Initially, they were weak and fairly sporadic, but as the count rate increased they became more regular, more closely spaced, and deeper (9%–16%), dominating the light curve (Fig. 3). Toward the end of the shoulder, the depth and the frequency of these dips started to decrease. In the power density spectrum, these dips show up as a QPO peak near 0.1 Hz and occasionally its harmonic (see Fig. 2*b*). The underlying power density spectrum is again modeled as a broken power law, but the power density spectrum below the break (generally at 0.1–0.8 Hz) is not flat (index mostly 0.1–0.5). The noise amplitude is much weaker (4.6%–9.7% rms) than in the initial (A) observations. Three peaks are observed in the power density spectra, typically at 3–5 Hz (increasing with count rate), 6–8 Hz (no long-term trend with count rate), and near 13.5 Hz (roughly constant), with rms amplitudes of 7%–4%, 4%–1%, and ~2%, respectively. The amplitudes generally decreased with count rate and time. The QPO near 13.5 Hz is weak and can only be detected in our longer observations. Because of the gap in observations, we cannot tell if these three QPOs are the same as those seen in A. The highest frequency QPO has $Q \sim 9$. The Q (2–7) of the two lower frequency peaks is lower than the QPOs of A. This is especially true for the lowest frequency peak.

We find two observations (denoted as b in Fig. 1) outside the shoulder in which dipping behavior reappears, one near maximum (C) and the other on the decline (D). Within the

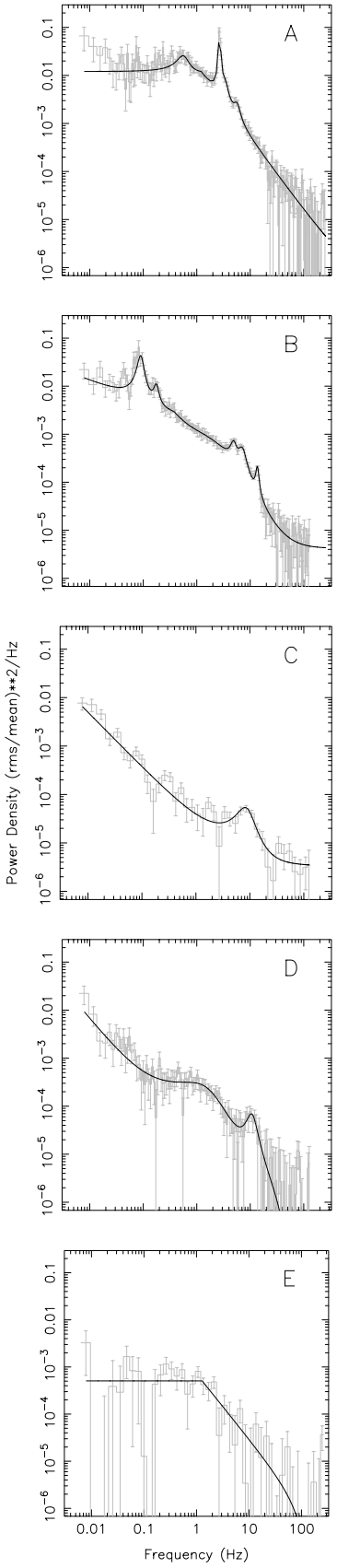

FIG. 2.—Representative power density spectra in chronological order through the 1998 outburst. Throughout the text the different types of timing behavior are referred to by their label within this figure, i.e., A, B, C, D, E.

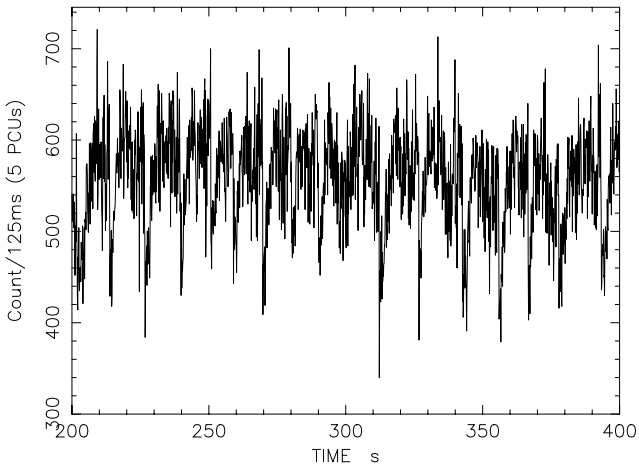

FIG. 3.—Light curve (Standard 1) over the ~2–~60 keV range showing the dipping behavior in B. The observation was made on 1998 February 13 (TJD 50,857).

Tomsick & Kaaret data set, there is at least one further instance where dipping reappears on the decline. This observation was made on the day preceding our observation showing dips on the decline (b). In each case the count rate and color (spectra) become comparable to those in the plateau (B).

We investigated the behavior of the QPOs in and outside the dips using 1 and 2 s data segments sorted by count rate. We found that the ~13.5 Hz QPO remained constant in amplitude and frequency. However, the QPO peak with a frequency near 6–8 Hz dropped in frequency to ~4.5 Hz within the dips while remaining at a similar amplitude. There are only two QPOs: one stable near 13.5 Hz and the other moving from 6–8 Hz outside the dips to 4–5 Hz. This explains the three peaks in Figure 2*b* at 13.6, 7, and 5 Hz. The width of the QPO peaks is larger than just that expected from the QPO being truncated on entering and leaving the dips. This is consistent with either the frequency varying or the wave trains that make up the lower frequency QPO being in general shorter than the dips, i.e., less than 5 s.

Behavior C.—On about 1998 February 18 (TJD 10,863, Fig. 1), the ASM/PCA count rate increases rapidly (<1 day), reaching a broad roughly constant maximum until February 24 (TJD 10,869), after which the count rate drops rapidly. Here there are no dips, and the power density spectrum shows weak (0.5%–2.3%), broad (few Hz) QPO with frequencies in the 6.5–9.5 Hz range superimposed upon a power-law (slope 1.0–1.9) continuum (1.4%–2.7% rms) (see Fig. 2*c*). Occasionally, an extra (<2% rms) Lorentzian component peaking in the 1–2 Hz range was required in the fits. This peak is similar to the marginal QPO detection of Kuulkers et al. (1998).

Behavior D.—After the sharp drop (≤1 day) on TJD 10,869, the flux continues to decline with count rates ranging from those of B to A. The power density spectrum shows a broad bump near 1 Hz, a steep component at very low (<0.1 Hz) frequencies, and a 2% rms amplitude QPO peak near 11 Hz. Note that this steep component is similar in amplitude and slope to the power-law component of C. The broadband noise was modeled with either a flat-topped, broken power law with a break near 1 Hz and a

TABLE 1

BROADBAND NOISE AND QPO FIT PARAMETERS

	NOISE FIT PARAMETERS					QPO FIT PARAMETERS		
BEHAVIOR	Count Rate (counts s^{-1} 5PCUs^{-1})	Percent rms (0.01–100 Hz)	ν_{break}	$\alpha < \nu_{break}$	$\alpha > \nu_{break}$	Percent rms	FWHM (Hz)	Frequency (Hz)
A	1426.34	20.36 ± 0.35	0.97 ± 0.04	0.0 Fixed	$1.45^{+0.03}_{-0.07}$	$17.03^{+0.18}_{-0.38}$	$0.2113^{+0.006}_{-0.015}$	$2.677^{+0.0045}_{-0.0054}$
						$7.93^{+0.66}_{-0.83}$	0.95 ± 0.013	$3.33^{+0.06}_{-0.15}$
						$5.79^{+0.41}_{-0.48}$	$1.49^{+0.19}_{-0.22}$	5.60 ± 0.05
B	4710.90	$6.61^{+0.13}_{-0.12}$	$2.26^{+0.10}_{-0.14}$	$0.51^{+0.048}_{-0.082}$	$1.78^{+0.19}_{-0.14}$	$2.876^{+0.041}_{-0.050}$	1.072 ± 0.045	4.953 ± 0.017
						$4.340^{+0.032}_{-0.070}$	$3.321^{+0.065}_{-0.075}$	$7.048^{+0.030}_{-0.033}$
						$2.035^{+0.029}_{-0.0485}$	$1.628^{+0.060}_{-0.100}$	$13.674^{+0.022}_{-0.018}$
C	5803.61	$1.63^{+0.15}_{-0.13}$			$1.13^{+0.09}_{-0.08}$	$2.29^{+0.25}_{-0.19}$	$6.9^{+2.1}_{-1.5}$	$8.16^{+0.45}_{-0.50}$
D	3724.48	$1.35^{+0.35}_{-0.22}$			$1.35^{+0.27}_{-0.20}$	$3.65^{+0.38}_{-0.34}$	$2.92^{+0.46}_{-0.42}$	$0.80^{+0.20}_{-0.28}$
						$2.28^{+0.27}_{-0.22}$	$5.26^{+1.66}_{-1.21}$	$10.54^{+0.52}_{-0.50}$
	3724.48	$3.24^{+0.28}_{-0.22}$	$1.39^{+0.13}_{-0.13}$	0.0 Fixed	$1.585^{+0.25}_{-0.23}$	$1.80^{+0.15}_{-0.15}$	$0.0539^{+0.0178}_{-0.0168}$	0.0 Fixed
						$2.11^{+0.32}_{-0.25}$	$4.8^{+1.7}_{-1.2}$	$10.59^{+0.53}_{-0.51}$
E	893.21	$4.50^{+0.66}_{-0.75}$	$1.28^{+0.78}_{-0.24}$	0.0 Fixed	$1.38^{+1.915}_{-0.28}$			

NOTES.—The broadband noise and QPO fit parameters of the five representative power density spectra shown in Fig. 2. A broken power law is used for A, B, and E, and a power law is used for C to model the broadband noise. Lorentzian peaks are used to model any QPO peaks and broader "bumps." For A, a 0.34 FWHM bump at 0.55 Hz with 8.8% rms amplitude can be added but only for the first observation. For D two equivalent models were used: (top) a power law with a "bump" and a QPO and (bottom) a broken power law with a zero-frequency Lorentzian and QPO. The "bump" and zero-frequency Lorentzian can be considered extra components of the broadband noise. The errors are the 1 σ single-parameter error, i.e., the parameter range within $\Delta\chi^2 = 1.0$ of the best-fit minimum.

zero-frequency Lorentzian or by a power law and a broad Lorentzian peak near 1 Hz (see Fig. 2*d*). The broad bump contributed 2.4%–4.4% rms, generally increasing as flux declined. The very low frequency component became generally weaker (maximum 1.8% rms) as 4U 1630−47 faded. This sort of power density spectrum persisted even as the count rate dropped to levels where large-amplitude QPOs (A) were observed on the rise. The colors in these decline observations are different from those of the same flux on the rise.

Behavior E.—In the last two observations beyond TJD 10,850, the very low frequency component disappears and the power density spectrum can be well fit by just a flat-topped broken power law. The change from D to E seems to be gradual and continuous. The break frequency is near 1 Hz, the slope above the break is ~ 1.5, and the amplitude is $\sim 3\%$ rms. This flat-topped noise is very similar to the ~ 1 Hz bump seen on the decline (D) and could well be the same component. The absorbed flux (2–10 keV) in our last observation (TJD 10,873) is 1.9×10^{-9} ergs cm^{-2} s^{-1}.

Behavior F.—Much later (at TJD 10,950), Tomsick & Kaaret (2000) report a marked change in the power density spectra, from spectra with $\lesssim 4\%$ rms noise (like E) to spectra with more than 10% rms broadband noise and a single 3.38 Hz QPO with 9% rms amplitude. The QPO frequency decreased to about 0.2 Hz as 4U 1630−47 faded to an absorbed flux (2–10 keV) of $\sim 3 \times 10^{-10}$ ergs cm^{-2} s^{-1} at TJD 10,972 (their last observation and last scheduled for *RXTE*).

Eighteen days later (1998 June 26, TJD 10,990) during an *RXTE* PCA observation of SGR 1627−41 that included 4U 1630−47 within the field of view (FOV; response 37%), 0.15 Hz QPOs were found (Dieters et al. 1998b). The amplitude was at least 3% rms. The actual amplitude is dependent upon the relative contributions to the flux from SGR 1627−41, 4U 1630−47, and the local Galactic ridge emission. Given that *BeppoSAX* observations made on the 1998 August 7 (TJD 11,032) and 1998 September 16 (TJD 11,072) show that 4U 1630−47 was still much brighter than SGR 1627−41 and that SGR 1627−41 was in quiescence and hence fainter (Woods et al. 1999), while Tomsick & Kaaret (2000) found 3.4–0.2 Hz QPO, it is reasonable to suppose that the 0.15 Hz QPO originate from 4U 1630−47. Thus, the amplitude of the 0.15 Hz QPO must be at least 8.2% rms.

3.2. *Spectral Evolution*

For each observation, the energy spectrum is modeled with the combination of a multicolor disk component and a power-law component, which is typical for black hole candidates (Tanaka & Lewin 1995). Such parameterization can adequately describe the observed X-ray spectrum of 4U 1630−47, although an additional Gaussian component is always required, probably indicating the presence of an iron Kα line. Significant residuals still remain in some cases (especially C and D), but the results are good enough to provide a rough description of the spectral evolution of the source during the outburst. More detailed spectral results and discussions will be presented elsewhere. The decline is also partially covered by *BeppoSAX* observations (Oosterbroek et al. 1998; their observations 1–5 occur when we find 4U 1630−47 in behaviors to C, C, D or possibly b, D, E, respectively).

Following the onset of the outburst (the first four observations, covering A and the transition into B), both the soft component and the power-law component strengthen. Initially, (A) the soft component is the weaker, contributing $\lesssim 20\%$ of the total unabsorbed (1.5–60 keV) flux. At the same time, the power law steepens (the photon index goes from -2.0 to -2.5) as shown by the changes in the color-color diagram of Figure 1. This is consistent with the results from simultaneous ASM and BATSE observations (Hjellming et al. 1999). During B, the two components both grow in strength with each contributing about half the unabsorbed flux.

Moving to C, the absorption increases [9–10 as opposed

to (8–8.5) $\times 10^{22}$ atoms cm^{-2}] and the power-law component becomes stronger ($\sim$60% unabsorbed) relative to the soft (disk) component. As C progresses, the power-law component weakens and becomes steeper (photon index becomes as steep as -2.8). The combination of higher absorption and steepening power law move 4U 1630−47 away from the pure power laws toward the pure blackbody curves on the color-color diagram (Fig. 1).

The decaying period (D and E) begins with the soft component contributing most of the unabsorbed flux (60%–70%) at a somewhat lower temperature ($kT = 1.2$ keV rather than 1.4–1.5 keV of C). As the count rate drops, the absorption also drops, the soft component weakens and becomes softer, while the power-law component flattens. In E the soft component contributes at most 45%–55% of the unabsorbed flux, the absorption is (4–7) $\times 10^{22}$ atoms cm^{-2}, and the power law index is ~ -2. This combination of changes moves 4U 1630−47 to the right and lower on the color-color diagram (Fig. 1). These trends continue in F, with the soft component contributing at most 10% of the unabsorbed 2–60 keV flux, the power-law index being in the range -1.4 to -1.8, and the absorption being a little lower still. Thus, the energy spectra indicate a further hardening of the source, i.e., more like A.

3.3. *The BeppoSAX Data*

Behavior G.—The *BeppoSAX* MECS (2 and 3) PHA spectra can be adequately fit (August: reduced $\chi^2 = 0.8757$ with 92 degrees of freedom [dof]; September: reduced $\chi^2 = 1.5168$ with 92 dof) with a simple absorbed power-law model. We used three- and four-channel rebinning over the 1.8–11.5 keV range. The best-fit parameters for 1998 August 7 (TJD 11,032) and 1998 September 16 (TJD 11,072) are $N_{\rm H} = (7.7 \pm 0.45) \times 10^{22}$ and $(8.1 \pm 0.7) \times 10^{22}$ atoms cm^{-2}, $\Gamma = 1.42 \pm 0.07$ and 1.6 ± 0.25, with absorbed fluxes (2–10 keV) of 1.7×10^{-10} and 0.98×10^{-10} ergs cm^{-2} s^{-1}, respectively. These fluxes indicate a steady and long-term decline in the brightness of 4U 1630−47 (Tomsick & Kaaret 2000). Using an assumed distance of 10 kpc, the latter flux corresponds to a luminosity of 1.2×10^{36} ergs s^{-1}. Using the same energy range (2–2.4 keV) and absorption (0.2×10^{22} atoms cm^{-2}) as Parmar et al. (1997), we find the luminosity in September to be 6×10^{36} ergs s^{-1}. This is much brighter than the quiescent levels found by Parmar et al. (1997).

We calculated power density spectra for each *BeppoSAX* observation for the source and background. Of the two observations, only the August observation had significant ($>5\ \sigma$) excess power. At this time there was at least 50% rms variability (4U 1630−47 and background) over the 0.004–128 Hz range. Most of the excess is below 5 Hz. The background (7% of the source count rate) could contribute at most (3 σ upper limit) 10% rms to the source variability. Therefore, 4U 1630−47 had at least 40% rms variability in the 0.004–128 Hz range. The combination of high rms variability and a power-law energy spectrum indicates that 4U 1630−47 had entered the low state.

4. DISCUSSION

As compared to previous observations of 4U 1630−47, what is surprising about the 1998 outburst is the sheer variety of timing behavior. We can tentatively link some of the QPOs seen from 4U 1630−47. The large-amplitude QPO seen on the early rise (A) is similar in behavior to the 0.1–10 Hz QPO on the early rise of XTE J1550−564 (Cui et al. 1999). In both cases hard X-ray flux as seen by BATSE is declining and the spectrum in the PCA is softening. The 3.7–0.2 Hz QPO seen late in the outburst (F) by Tomsick & Kaaret (2000) and a 0.15 Hz QPO seen later by Dieters et al. (1998b) would be the same but in reverse. Given the evolution of the spectrum (soft to hard), this is reasonable. Finally, the large-amplitude QPO seen on the early rise of the 1999 mini(?)outburst (McCollough et al. 1999), would also be the similar type of QPO. In all cases the shape and amplitude of the broadband noise is similar. However, the harmonic content of the decline QPO and those in 1999 are different from those on the rise. The appearance of these large-amplitude QPOs with strong, flat-topped noise cannot depend solely on mass accretion rate as measured by count rate since they do not reappear during the decline D. These QPOs could well only appear in a restricted range in the color-color diagram and therefore of spectral parameters. Unfortunately, we cannot link the QPOs of A with those of B as would be suggested by the analogy with XTE J1550−564, which showed QPOs changing continuously from 0.1 to 10 Hz.

The quasi-periodic dips of B and b appear only when 4U 1630−47 is within a fairly narrow range of count rate and hardness. Their increase and then decrease in depth and frequency as the count rate and color-color diagram position steadily changes in B indicates that there are some optimum conditions for their occurrence. The pair of QPOs, one stable at 13.5 Hz and the other with a count rate/frequency dependence, are associated with the same conditions since they reappear in the b observations which are B-like excursions from C or D where neither QPO are present.

The 1998 outburst of 4U 1630−47 was clearly very complex. According to the canonical model for black hole transients, as a function of increasing accretion rate a source should pass through the states in this order: LS/IS/HS/VHS, and of course in reverse order as accretion rate decreases again toward quiescence. As a first approximation, we can infer accretion rate from the observed X-ray flux, although this approach has to be followed carefully. During the course of our observations, covering most of the rise and decline (A through E), there is always a mixture of a soft and hard component.

At the beginning of the outburst (A), at a relatively low accretion rate, the colors indicate that the source is rather hard, with the energy spectrum dominated by a power-law component (see Fig. 1), i.e., the soft component is less than 20% of the flux. The power density spectrum is similar to that of an IS (Belloni et al. 1997b), although the break frequency of the broadband noise component is rather low, possibly connected to the fact that these observations are made early in the outburst, when the source was probably moving from an LS to an IS.

Rather rapidly, the source increased in flux and moved to observations of type B. There is a transition period as both the relative contribution of the soft flux increases and the dipping behavior becomes established. Through B the soft flux increases due to a combination of steepening in the power law and an increase in the flux from the soft spectral component. But at no time does the soft component dominate the flux. The power density spectrum is extremely

complex and not easy to interpret. The dipping behavior is unlike the absorption dip(s) reported during the 1996 outburst. Superficially, the dipping behavior appears like that of GRS 1915+105 (Belloni et al. 1997b) and GRO 1655−40 (Remillard et al. 1999) for which the evidence is that the dips are due to a disk instability. However, note that another and different type of dip is present for GRS 1915+105 (Belloni et al. 2000). Alternatively, the dips of 4U 1630−47 may be more like dips and "flip-flops" seen in the VHS of GX 339−4 (Miyamoto et al. 1991). A detailed comparison among these various dipping behaviors is needed. In addition, there are three peaks in the power density spectrum: one from a stable QPO near 13.5 Hz and the other two from an intensity-dependent QPO. The difference in QPO behavior with count rate suggests that the two QPOs have different origins. There are numerous examples of QPO in this range, but only those of GRO 1655−40 show a combination of stationary and moving QPO (Remillard et al. 1999). However, the energy spectrum of GRO 1655−40 at this time shows the soft component dominating (like VHS), and there were no dips. The combination of dips and QPO initially suggests that type B behavior is a VHS, but unlike the canonical VHS the soft component does not dominate the flux, and it is not the highest flux regime. Overall, these "shoulder" observations do not fit in a clear way any of the canonical states and seem to be peculiar.

Next, the source jumps to C and, in terms of the broadband noise, into an obvious HS. The power-law shape, its slope, and amplitude are a good match to high states in both 4U 1630−47 and other BHCs. The QPO is so weak that it could well have escaped detection by previous instruments. They are similar to those seen from GRS 1915+105 in the "soft branch" (Chen, Swank, & Taam 1997). However, the spectrum indicates a strong power-law component contributing $\sim 60\%$ of the unabsorbed flux which is unlike an HS. The transitions in and out of C are both ≤ 1 day and among the most rapid ever seen.

The exit from C into D is marked as a drop in count rate, softening of the disk (soft) component, and a lowering of the absorption. Initially, the soft component contributes most of the flux (60%–70%), but this contribution declines as the count rate drops. Also, the power law hardens. The power density spectra (see Fig. 2*d*) are not unlike some observed in GX 339-4 in its VHS (Miyamoto et al. 1991, i.e., their Fig. 4*b*). Since the fluxes are lower in D and follow a probable HS, we can exclude a VHS, and it is natural to identify these observations with an IS, which is known to show characteristics very similar to those of the VHS (van der Klis 1995). The changes in the spectrum (HS-like toward LS-like) and color-color diagram support the identification with an IS.

At later times (E), the power density spectra are not very detailed due to the lower statistics but are similar to the IS spectra reported by Belloni et al. (1997a) and Méndez & van der Klis (1997). The colors and spectra indicate that the soft component decreased in relative strength and softened further as the power law flattened. The source seems to be on its way, via the reappearance of strong QPO and strong broadband noise, to the LS (high rms, power-law energy spectrum), which was reached by the time of the *BeppoSAX* observations (G) well below the detection threshold of the PCA but much brighter than the quiescent emission (Parmar et al. 1997).

On the rise, the spectral evolution, the QPOs, and their frequency evolution are very similar to that of XTE J1550−564 (Cui et al. 1999). This may not be that surprising given that both these sources have been caught very early in their outbursts. In the past the wealth of information found during the rise phases of the outburst have been missed. The changes in spectrum (soft to hard) on the decline are similar to that of many transients. However, the power density spectra are unusual. They are similar to that of Cir X-1 as it moves from the "upper banana" (similar to HS) through the "lower banana" into an extreme "island state" (similar to LS) (Oosterbroek et al. 1995). This serves as a warning that the spectral/timing properties discussed here and for other sources are not unique to BHCs.

This work supported by NASA/LTSA NAG 5-6021 (Dieters, van Paradijs, Kouveliotou, and Lewin), NAG 5-7483 (Dieters), NAG 5-7484 (Cui), and the Netherlands Organization for Scientific research (NWO) under grants 614-51-002 and Spinoza-08-0.

REFERENCES

Barret, D., McClintock, J. E., & Grindlay, J. E. 1996, ApJ, 473, 963
Belloni, T., & Hasinger, G. 1990, A&A, 227, L33
Belloni, T., Klein-Wolt, M., Méndez, M., van der Klis, M., & van Paradijs, J. 2000, A&A, 355, 271
Belloni, T., Méndez, M., King, A. R., van der Klis, M., & van Paradijs J. 1997a, ApJ, 479, L145
Belloni, T., Méndez, M., van der Klis, M., Hasinger, G., Lewin, W. H. G., & van Paradijs, J. 1996, ApJ, 472, L107
Belloni T., van der Klis, M., Lewin, W. H. G., van Paradijs, J., Dotani, T., Mitsuda, K., & Miyamoto, S. 1997b, A&A, 322, 857
Boella, G., et al. 1997, A&AS, 122, 327
Chen, X., Swank, J., & Taam, R. E. 1997, ApJ, 477, L41
Cui, W. 1999, in ASP Conf. Ser. 161, High Energy Processes in Accreting Black Holes, ed. J. Poutanen & R. Svensson (San Francisco: ASP), 97
Cui, W., Zhang, S. N., Chen, W., & Morgan, E. H. 1999, ApJ, 512, L43
Cui, W., Zhang, S. N., Focke, W., & Swank, J. H. 1997, ApJ, 484, 383
Dieters, S. W., Belloni, T., Kuulkers, E., Harmon, A. B., & Woods, P. M. 1998a, IAU Circ. 6823
Dieters, S. W., Woods, P., Kouveliotou, C., & van Paradijs, J. 1998b, IAU Circ. 6962
Gilfanov, M., et al. 1994, in The Lives of Neutron Stars, ed. M. A. Alpar, Ü. Kiziloglu, & J. van Paradijs (NATO ASI Ser. C, 450; Dordrecht: Kluwer), 351
Hjellming, R. M., et al. 1999, ApJ, 514, 383
Jahoda, K., Swank, J. H., Giles, A. B., Stark, M. J., Strohmayer, T., Zhang, W., & Morgan, E. H. 1996, Proc. SPIE, 2808, 59
Jones, C., Forman, W., Tananbaum, H., & Turner, M. J. L. 1976, ApJ, 210, L9
Kuulkers, E., Parmar, A. N., Kitamoto, S., Cominsky, L. R., & Sood, R. K. 1997a, MNRAS, 291, 81
Kuulkers, E., van der Klis, M., & Parmar, A. N. 1997b, ApJ, 474, L47
Kuulkers, E., Wijnands, R., Belloni, T., Méndez, M., van der Klis, M., & van Paradijs, J. 1998, ApJ, 494, 753
Levine, A. M., et al. 1996, ApJ, 469, L33
McCollough, M. L., Harmon, B. A., Dieters, S. W., & Wijnands, R. 1999, IAU Circ. 7165
Méndez, M., Belloni, T., & van der Klis, M. 1998, ApJ, 499, L187
Méndez, M., & van der Klis, M. 1997, ApJ, 479, 926
Miyamoto, S., Kimura, K., Kitamoto, S., Dotani, T., & Ebisawa, K. 1991, ApJ, 383, 784
Oosterbroek, T., Parmar, A. N., Kuulkers, E., Belloni, T., van der Klis, M., Frontera, F., & Santangelo, A. 1998, A&A, 340, 431
Oosterbroek, T., van der Klis, M., Kuulkers, E., van Paradijs, J., & Lewin, W. H. G. 1995, A&A, 297, 141
Parmar, A. N., Stella, L., & White, N. E. 1986, ApJ, 304, 664
Parmar, A. N., Williams, O. R., Kuulkers, E., Angellini, L., & White, N. E. 1997, A&A, 319, 855
Priedhorsky, W. C. 1986, Ap&SS, 126, 89

Remillard, R. A., Morgan, E. H., McClintock, J. E., Bailyn, C. D., & Orosz, J. A. 1999, ApJ, 522, 397
Rutledge, R. E., et al. 1999, ApJS, 124, 265
Tanaka, Y., & Lewin, W. H. G. 1995, in X-Ray Binaries, ed. W. H. G. Lewin, J. van Paradijs, & E. P. J. van den Heuvel (Cambridge: Cambridge Univ. Press), 126
Tomsick, J. A., & Kaaret, P. 2000, ApJ, 537, 448
Tomsick, J. A., Lapshov, I., & Kaaret, P. 1998, ApJ, 494, 747
van der Klis, M. 1995, in X-Ray Binaries, ed. W. H. G. Lewin, J. van Paradijs, & E. P. J. van den Heuvel (Cambridge: Cambridge Univ. Press), 252
Woods, P. M., et al. 1999, ApJ, 519, L139
Zhang, W. 1995, *XTE*/PCA Internal Memo 1995 May 23
Zhang, W., Jahoda, K., Swank, J. H., Morgan, E. H., & Giles, A. B. 1995, ApJ, 449, 930